THE IMPACT OF OPHIOLITIC MÉLANGES ON THE GROUNDWATER GEOCHEMISTRY OF NAEEN AQUIFER (CENTRAL IRAN)

Zahra Kayhomayoon

Department of Geology, Payame Noor University, Tehran, Iran.
✉ *Corresponding author, email: Zkayhomayoon@pnu.ac.ir*

Keywords: *Ophiolite mélange; hydrogeochemistry; statistical methods, artificial neural networks; Naeen; Iran.*

ABSTRACT

The management of groundwater resources requires recognizing the natural and human factors affecting water quality and, if possible, controlling, reducing, or eliminating the detrimental effects, if any. In order to investigate the effects of ophiolite mélange on the quantity and quality of water resources in the Naeen region, central Iran, the quantitative data of 34 observation wells in the time span between 2005 and 2020, the qualitative data of 20 groundwater samples from the Naeen aquifer, and 22 samples of groundwater from the Daghe Sorkh aquifer were investigated. Groundwater flow maps, aquifer hydrographs, compositional diagrams (Piper, Stiff, Scholler, and Wilcox diagrams), analytical diagrams, ionic ratios, saturation indices, statistical analyses (correlation matrix, dendrogram, hierarchical cluster analysis), and neural networks self-organizing maps (SOM) were considered for quantitative and qualitative analyse of the Naeen and Daghe Sorkh aquifers. Based on the quantitative investigations of the Naeen aquifer, the drainage of four permanent Qanats located in the south of the ophiolitic massif is affected by structural features (fractures and faults), Cretaceous limestones, and alluvial fans in the northern high-elevation regions of the aquifer. Analyses of the qualitative data showed that cation exchange, carbonate dissolution, and silicate weathering are the dominant processes affecting groundwater chemistry. Alteration and dissolution of peridotites (chiefly dunites and harzburgites) of the ophiolitic complex are responsible for the transfer of magnesium and bicarbonate to the groundwater interacting with the ophiolitic rocks. The fineness of aquifer sediments, and consequently, the increase in residence time, the high amount of evaporation compared to rainfall in the study area, and the return of agricultural water with very high salinity have caused an increase in EC values of the groundwater in the study aquifer.

INTRODUCTION

Ophiolitic rocks cover about one percent of the earth's surface. These rocks are the remains of the ancient oceanic crust and the upper mantle, which are widespread on the surface of continents along the tectonic suture zones (Lods et al., 2020 and references therein). Ophiolitic mélanges are the result of severe tectonic deformation and mixing of rock materials in trenches (Hamilton, 1969; Dewey and Bird, 1971; Hall, 1976). Ophiolites show evidence of magmatic, tectonic, and hydrothermal processes related to seafloor spreading. Therefore, these rocks are the best archives of the history of the evolution of ocean basins from the rift-drift and seafloor spreading stages to subduction initiation and final closure (Dilek and Furnes, 2014). Ophiolitic formations are effective in controlling the quantity and quality of groundwater resources in many regions. Studies show that the structural heterogeneities of these rocks, caused by the presence of different lithological units and multi-scale hydraulic discontinuities, lead to complex hydrogeological features that are not yet well defined (Lods et al., 2020).

The high reactivity of minerals in ultramafic and mafic rocks in ophiolites has a great effect on the chemical composition of groundwater, so it becomes unsuitable for human consumption in many aquifers. Accordingly, the quality of water for different uses has changed. The effect of ophiolites on groundwater quality has been investigated all over the world, including Australia (Gray 2003), Brazil (Bertolo et al., 2011a; 2011b), Cyprus (Neal and Shand, 2010), Greece (Moraetis et al., 2012; Dermatas et al., 2015; Kaprara et al., 2015; Kazakis et al., 2015; 2017; Kelepertzis and Tziritis, 2015; Dokou et al., 2016; Pyrgaki et al., 2021), Indonesia and Japan (Saputro et al., 2014), Italy (Bruni et al. 2002; Fantoni et al., 2002; Boschetti, et al., 2008; Apollaro et al., 2011; 2019; Margiotta et al., 2012; Lelli et al., 2014; Critelli et al., 2015; Paternoster et al., 2021,), Mexico (Robles-Camacho and Armienta, 2000), Oman (Vankeuren et al., 2019), Pakistan (Naseem et al., 2010), Serbia (Nikic et al., 2013), Turkey (Güler et al., 2017), United Arab Emirates (Wood et al., 2010), and USA (Robertson, 1975; Ball and Izbicki, 2004; Henrie et al., 2004; Gonzalez et al., 2005; Izbicki et al., 2008; Ndung'u et al., 2010; Mills et al., 2011).

According to the geological and tectonic conditions, Iran's ophiolites are mainly composed of the mélange type and are exposed in the form of narrow and more or less continuous strips along the main longitudinal faults. In terms of geographical distribution, Iran's ophiolites are divided into four groups: 1- ophiolites in northern Iran along the Alborz Mountain range, 2- ophiolites along the Zagros seam from Khoi to Kermanshah and Neyriz, 3- ophiolites in Makran, and 4- ophiolites and mélanges around the central microplate of Iran, including the Shahr-e Babak, Naeen, Sabzevar, and Nehbandan-Chelkore (Stocklin, 1968; Takin and Furnes, 1972). The effect of these rocks on the quality of groundwater has been studied in Khoi, Baft, Birjand, Sabzevar, Marivan, Torbat, and Firuzabad aquifers (Hajizadeh et al. 2011; Khaledi and Mohammadzadeh, 2012; Fazlnia et al., 2012; Nematollahi et al. 2016; Zamani et al., 2018; Mardani T., 2018, Majidi et al., 2019).

The impact of the Naeen mélange ophiolite, located in central Iran, on the quantity and quality of groundwater resources in the region has not been investigated so far. Therefore, in the present study, an attempt has been made to analyze the impact of the aforementioned rocks on the water resources of the region through the analysis of both quantitative and qualitative data.

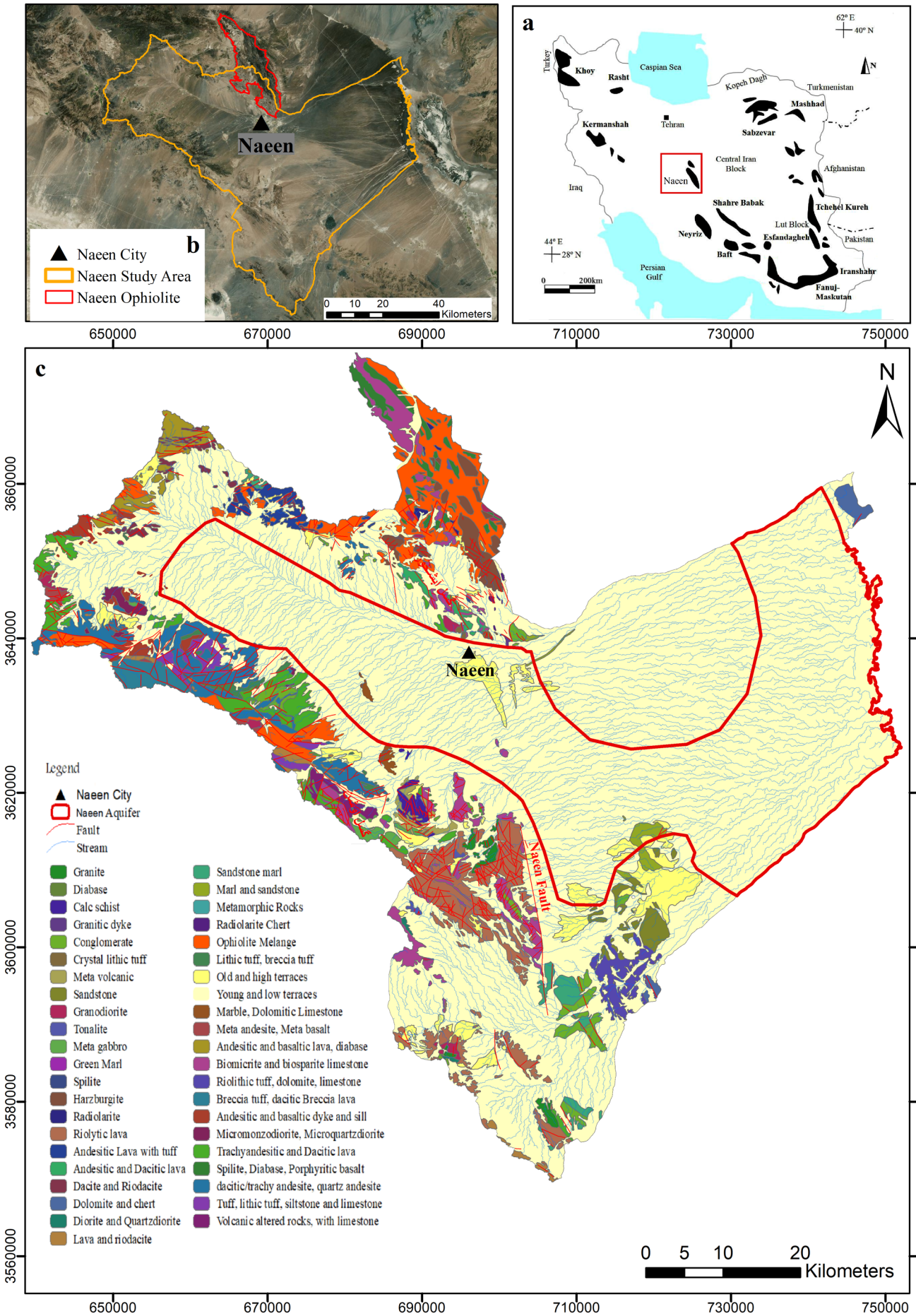

Fig. 1 - Geographical location and geological map of the Naeen area. The reader is referred to the PDF online for a colour version.

STUDY AREA

The Naeen mélange ophiolite, with an area of 600 km^2, is located in the north of the city of Naeen and is part of the ophiolite belt of the central micro-plate of Iran (Fig. 1). With its SSE-NNW direction, the ophiolitic sequence is the border of the central Iran domain with the Urumieh-Dokhtar magmatic arc, which crops out along the main Dehshir-Baft-Naeen fault (Aghanabati, 2004). The Naeen mélange ophiolite is composed of metamorphosed peridotite, pyroxene gabbro, gabbronorite, amphibole gabbro, plagiogranite, sheeted dykes, pillow lavas, and pelagic limestones of the Later Cretaceous along with quartzose shale and radiolarian cherts (Jabari, 1997). The ophiolitic sequence is pushed by a reverse fault on Eocene Flysch sediments and Oligo-Miocene sediments (Moghadam et al., 2009; 2013; Mehdipour et al., 2011).

In addition to the ophiolitic sequence, the study area includes two other geological complexes (Fig. 1). One is constituted by the Paleozoic sedimentary rocks that crop out in the southeast and include siltstones, sandstones, dolomites, and crinoid limestones that have been metamorphosed in the greenschist facies. The other one comprises volcanic, igneous, and sedimentary rocks belonging to the Cretaceous and Paleocene and volcanoclastic sedimentary rocks of the Oligo-Miocene age (Alai and Foudazi, 2004). The Naeen Plain aquifer, with an area of 1858 km^2, is located in the subbasin of the Siah Kuh desert within the watershed of the central Iranian plateau. Due to the dry and desert climate in this region, the maximum monthly evaporation in the summer months reaches 500 mm, while the average monthly precipitation rarely exceeds 50 mm. Therefore, due to the lack of surface water flow in this area, groundwater resources have been the only source of water supply for the residents for a long time. The groundwater resources of the study area are used for drinking and agriculture and are obtained from springs, wells, and Qanats, each one consisting of a series of vertical tunnels similar to wells, connected by a slightly sloping underground channel.

The aquifer of the study area is hosted in alluvial sediments deriving from the erosion of igneous, metamorphic, and sedimentary rocks (limestones and dolomites). It is of free type and is found at depths varying from < 3 m to > 75 m. The thickness of the saturation zone in the Naeen aquifer varies from 36 to 153 m. The minimum and maximum transmissivity values of the aquifer are 150 and 615 $m^2 d^{-1}$, respectively. Both the hydraulic conductivity and transmissivity of the aquifer increase from the west to the east of the plain. The greater increase in transmissivity in the eastern half of the aquifer compared to the hydraulic conductivity is due to the greater increase in the thickness of the aquifer in this area. The changes in the storage coefficient values in the upper part of the aquifer show that the northeastern and central areas of the aquifer are composed of coarser particles compared to other areas, where fine-grained clay occurs. The minimum and maximum specific storage coefficients of the aquifer are 2.5% and 6%, respectively (Zharf Aab Tadbir Consulting Engineers, 2018).

MATERIAL AND METHODS

In order to quantitatively investigate the Naeen aquifer, the data from 34 observation wells available in this study area have been used to draw maps of groundwater flow and hydrographs of the aquifer from 2005 to 2020. The data from four meteorological stations have been used to investigate the changes in precipitation in the study area. There are 432 operating wells, 407 aqueducts, and 73 fountains in the Naeen region. The main drainage of the aquifer is done through Qanats.

Qualitative evaluation of the Naeen aquifer has been done through the data obtained from the chemical analysis of groundwater samples related to 18 Qanats (Q), one well (W), and one spring (S). Due to the small turbidity of the samples (< 1 NTU), the groundwater samples were not filtered. In each sample, pH and EC values were measured in the field using portable instruments (WTW). Ca, Mg, K, Na, Cl, SO_4, CO_3, HCO_3, TDS, and Total Hardness (TH) were determined based on APHA (2017) methods at the central laboratory of the Regional Water Company of Isfahan (Table 1).

The results of the chemical analysis of 22 groundwater samples were used in the qualitative investigations of the Daghe Sorkh aquifer. Meanwhile, the qualitative data of water sources in the study area have been interpreted by considering the results of different measurements of each sample and also the set of measurements performed in one sampling location or different sampling locations. Graphical methods and statistical analyses were used to analyze the obtained chemical data. In addition to controlling the results of quantitative measurements, these methods make it possible to find the likely origin of the chemical composition of water resources. Graphical methods for displaying data obtained from the measurement of water samples were used to identify samples with anomalies and to determine chemical trends. These graphical methods included combined charts, Piper, Stiff, Scholler, and Wilcox diagrams. The computational

Table 1 - Parameters and elements measured in Naeen groundwater samples.

	Parameter	Detection Limit	Analysis Method	Instrument
In field	**pH**	0.01	pH meter	WTW- pH 315i
	EC	1 µS cm^{-1}, 0.1	ECmeter	WTW - Cond 315i
In Lab	**Cl**	1.77 mg l^{-1}	Titration	–
	SO_4	0.5 mg l^{-1}	Spectrophotometer	Shimadzu - UV 190
	CO_3	1.5 mg l^{-1}	Titration	–
	HCO_3	3.05 mg l^{-1}	Titration	–
	TH	2.5 mg l^{-1}	Titration	–
	Ca, K, Mg, Na,	0.001 -200 µg l^{-1}	ICP-OES & MS	Perkin Elmer Sciex Elan

and statistical methods included specific ratios, hierarchical analyses, and self-organizing maps (SOMs). The saturation indices have been extracted through hydrogeochemical modeling using the PHREEQC software. Hierarchical analysis of samples (Q-mode) and parameters (R-mode) was conducted using Minitab software and neural network SOMs were programmed in the MATLAB programming environment. Fig. 2 shows the flowchart of the present study.

RESULTS AND DISCUSSION

Quantitative investigation of the Naeen aquifer

According to the contours of the groundwater level, the fronts of groundwater inflow are from the west, northwest, and southwest of the aquifer. After entering the aquifer, the groundwater flows to the southeast and is discharged from the eastern side of the aquifer to the Siah-Kuh desert (Fig. 3). According to the Iso-Depth maps, the lowest depth of the water table (< 3 m) is located in the west and center of the Naeen aquifer, whereas other areas of the aquifer have higher water table depths (> 70 m). The main drainage of the Naeen aquifer takes place through the existing Qanats. There are four permanent Qanats (Q16, Q17, Q18, and Q9) in the south and southwest of the ophiolitic mountain to the north of Naeen; the depth of their main wells is less than 50 m and their maximum outflow is 50 l s^{-1}.

The effectiveness of the above-mentioned Qanats, mainly used for irrigation, is due to the structural fractures and the presence of Cretaceous limestones along with karst cavities and alluvial fans in the northern mountains, as confirmed through qualitative investigations of groundwater in this research. The Naeen aquifer is recharged both by the mountains located in the west of the study area, where carbonates, igneous, and metamorphic rocks crop out, and the ridge in the north of the study area where the ophiolitic complexes crop out. The hydrograph of the Naeen aquifer, based on the data from the observation wells in the years 2005 to 2020, generally shows a decreasing trend, with an average water level drop of 2 m during the 15-year study period (Fig. 4). Due to this drop in the water level, almost half of the Qanats and wells and all the springs have dried up.

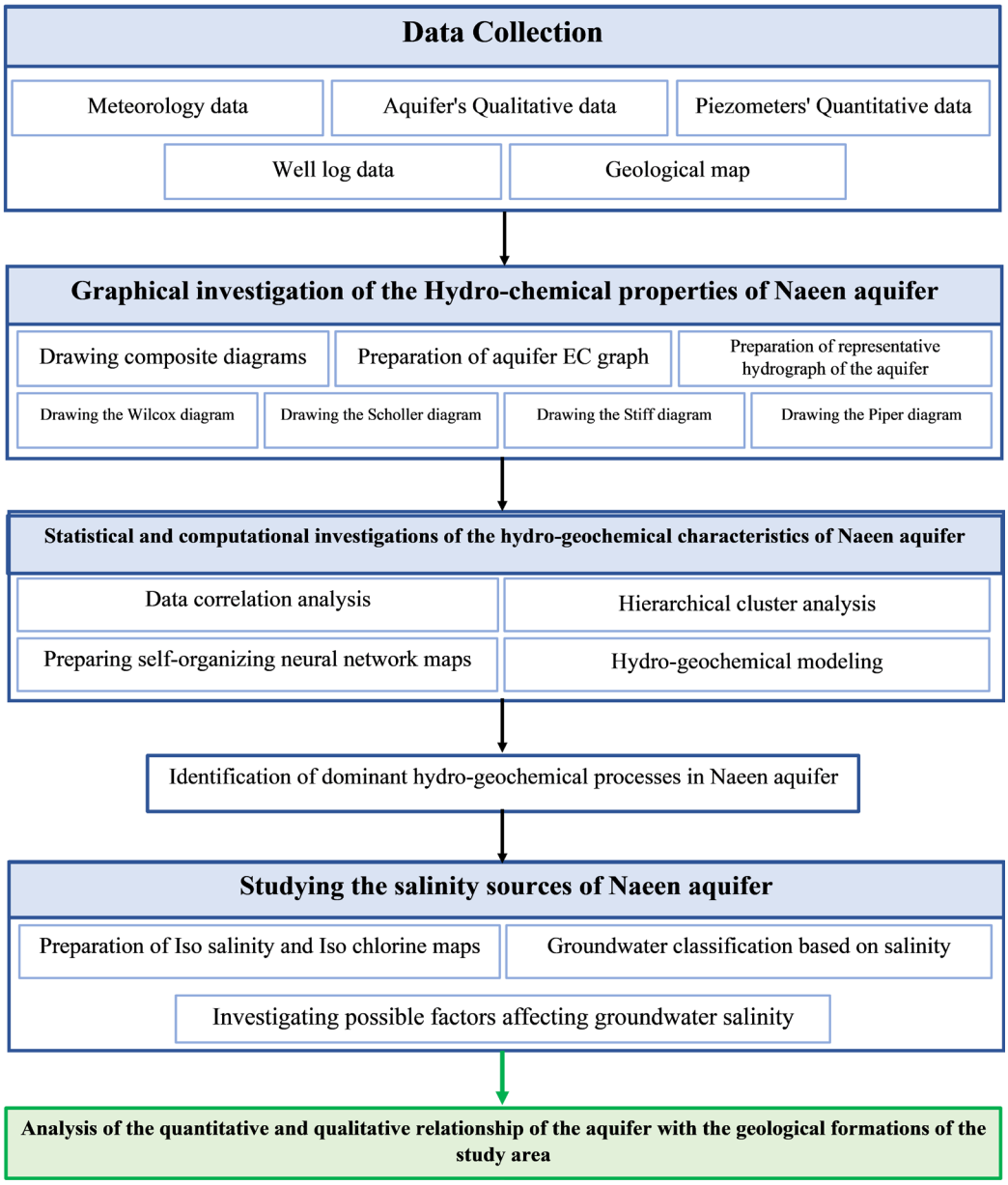

Fig. 2 - Flowchart of the present study.

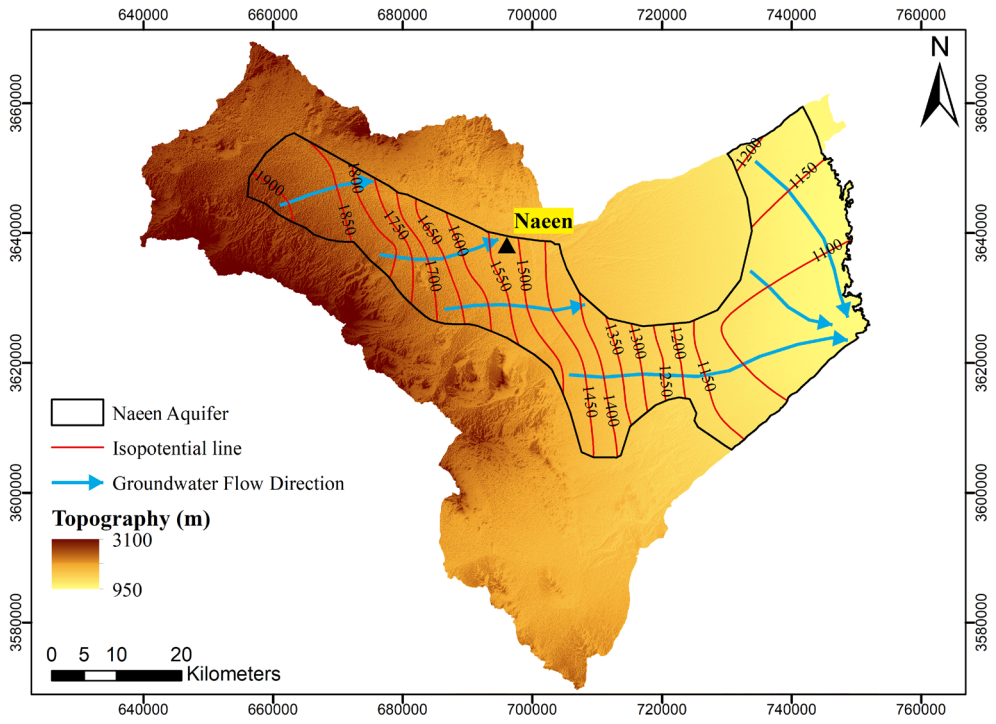

Fig. 3 - Groundwater flow direction map of the Naeen aquifer in 2020.

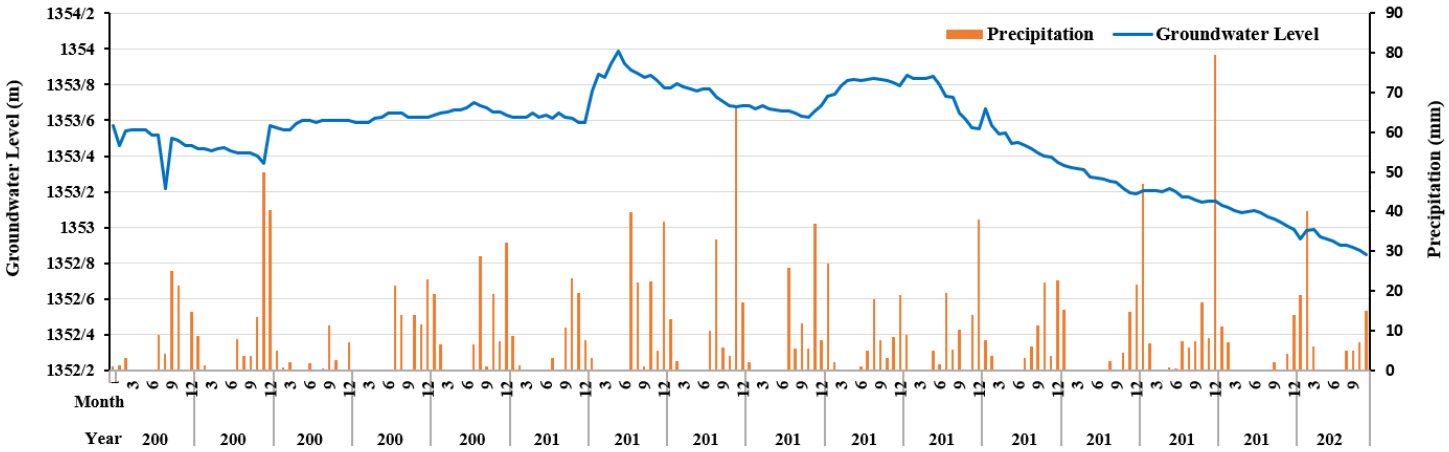

Fig. 4 - Hydrograph of the Naeen aquifer in a period from 2005 to 2020.

Qualitative investigation of the Naeen aquifer

The qualitative results of the Naeen study area, which were obtained during sampling in 2020, are presented in Table 2. Groundwater samples have been analyzed in the laboratory of the Isfahan Regional Water Company (ESRW). According to the laboratory protocol, charge unbalances < 5% are proportionally distributed among all solute concentrations and zero error is reported. Samples with a charge unbalance > 5% are reanalyzed.

pH and electrical conductivity (EC) values f the groundwater

The pH values of the groundwater in the Naeen aquifer range from 7.1 to 8.4. Half of the samples have pH values between 7.8 and 8.4, being relatively alkaline as typical of ophiolitic environments due to the limited development of soils and the consequently low production of CO_2 through organic matter decay. The reason for the moderate increase in pH values of groundwater in the study area is their low CO_2 partial pressure.

EC values of groundwater are in the range of 530 - 12700 mS cm^{-1}. Fig. 5, in which the EC and precipitation values in the years 2005 to 2020 are compared, shows that there is no clear relation between these two parameters. Significant changes are observed in precipitation, whereas EC is nearly constant. The difference between the maximum and minimum EC values is only 170 mS cm^{-1}, being equal to about 5% of the average value, which is similar to the EC measurement error.

Hydrogeochemical diagrams

Piper diagram. Based on the position of the samples in the Piper diagram (Fig. 6), the groundwater of the study area is represented in three groups: from Ca,Na-HCO_3 to Na,Ca-HCO_3, Na-SO_4,Cl and Na-Cl, apart from sample S which has an unusual Mg-Cl,SO_4 composition. The spread of samples

Table 2 - Qualitative results of the Naeen study area recorded in 2020 (concentration and sums of concentrations are in mEq l-1, <DL: below detection limit).

Name	Source	UTM-X	UTM-Y	K	Na	Mg	Ca	CO_3	SO_4	Cl	HCO_3	TDS (mgL^{-1})	pH (pH Unit)	TH (mgL^{-1} as $CaCO_3$)	EC (µS/cm)	∑Cations	∑Anions	Error
Q1	Qanat	644369	3642311	<DL	2.4	2.1	4.3	<DL	2	2.3	4.5	525	7.1	320	8.7	8.8	8.8	0
Q2	Qanat	646609	3644851	<DL	4.1	1.2	3	<DL	3	1.7	3.6	521	8	210	8.1	8.3	8.3	0
Q3	Qanat	652803	3638009	<DL	1.3	1	3.5	<DL	1.6	1	3.2	371	7.7	225	570	5.8	5.8	0
Q4	Qanat	660495	3641961	<DL	5.8	1.2	2.6	<DL	3.2	2.5	3.9	593	7.9	190	912	9.6	9.6	0
Q5	Qanat	662316	3635215	<DL	2.9	0.9	2.4	<DL	1.7	1.1	3.4	389	7.6	165	598	6.2	6.2	0
Q6	Qanat	664013	3635645	<DL	0.2	1.2	2.7	<DL	2.7	2.2	3.2	5.3	7.8	195	774	8.1	8.1	0
Q7	Qanat	664314	3639953	<DL	11.7	1.9	4.5	<DL	7	5.5	5.6	1189	7.8	320	1699	18.1	18.1	0
Q8	Qanat	676632	3624581	<DL	6.5	1.2	2.2	<DL	2.7	2.5	3.8	593	7.9	170	912	9	9	0
Q9	Qanat	677981	3644140	0.1	33.2	8.6	12.6	<DL	16.8	32.4	5.3	3500	7.6	1061	5000	54.5	54.5	0
Q10	Qanat	678785	3630961	<DL	3.5	0.9	2	0.4	2.3	1.3	2.4	412	8.4	145	634	6.4	6.4	0
Q11	Qanat	679623	3618003	<DL	2.3	1.5	1.7	<DL	1.4	1	3.1	345	7.9	160	531	5.5	5.5	0
Q12	Qanat	679690	3625508	0.1	6.3	0.1	3	<DL	3.7	2	3.7	568	8	155	875	9.4	9.5	0
Q13	Qanat	681252	3618798	<DL	13.3	2.5	3.9	<DL	8.6	6.4	4.7	1356	8	320	1937	19.7	19.7	0
Q14	Qanat	682743	3622774	<DL	6.1	1	2	<DL	3.6	2	3.5	575	8	150	884	9.1	9.1	0
Q15	Qanat	686079	3619401	<DL	19.8	3.8	4.6	<DL	14.2	8	6	1841	8	420	2630	28.2	28.2	0
Q16	Qanat	693945	3638725	0.2	45.6	7.7	16.8	<DL	21.5	45.1	3.7	4627	7.5	1226	6610	70.3	70.3	0
W	Well	694230	3637562	0.2	37.9	5.9	15.6	<DL	18.2	36.7	4.5	3718	7.6	1075	5720	59.4	59.6	0
S	Spring	696186	3651291	<DL	3.7	7.9	1.3	<DL	3.9	7.9	0.9	898	8.3	461	1283	12.9	12.7	0
Q17	Qanat	696905	3639838	0.1	43.4	12.8	19.2	<DL	19.3	52.8	3.4	4925	7.5	1602	7040	75.5	75.5	0
Q18	Qanat	700307	3638595	0.3	83.5	19	35	<DL	26	107.1	4.7	8883	7.4	2703	12690	137.8	137.8	0

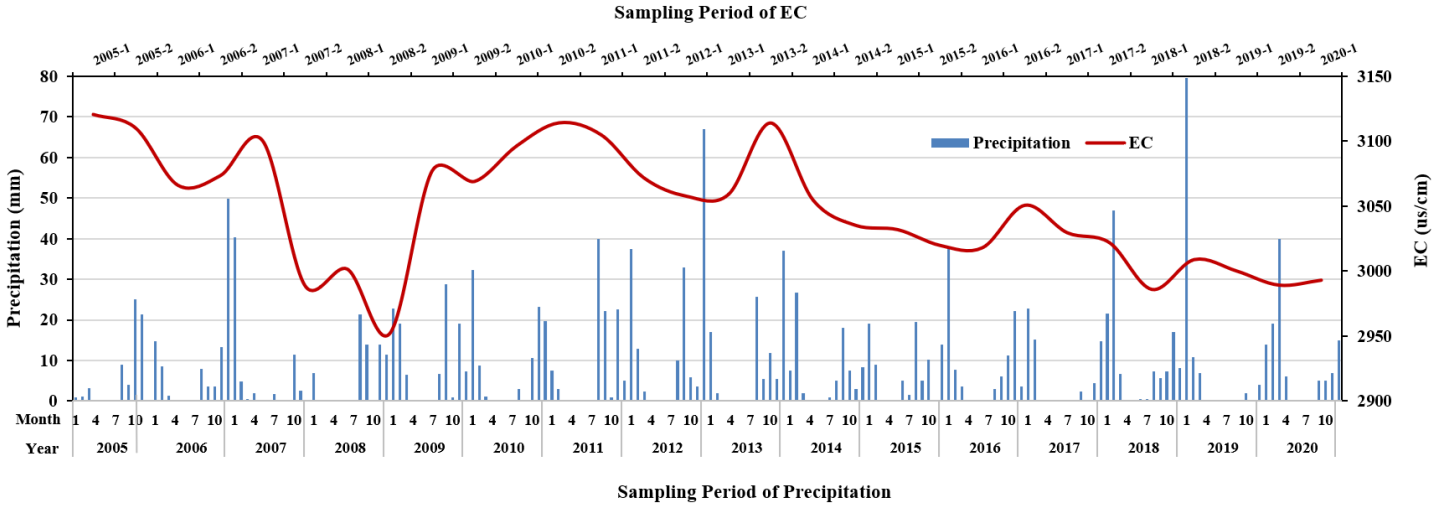

Fig. 5 - EC variations in the Naeen aquifer in a period from 2005 to 2020.

in the anion and cation triangles suggests that the hydrogeochemical evolution of the groundwater in the region is Ca,Na-HCO_3 → Na,Ca-HCO_3 → Na-SO_4,Cl → Na-Cl. The transition from Ca,Na-HCO_3 → Na,Ca-HCO_3 might be due to either cation exchange or dissolution of silicate rocks.

Stiff diagram. Based on isomorphic Stiff diagrams and concentration values of the main ions in the water samples, a total of 20 groundwater samples were divided into six main types of :

1- Ca-HCO_3: Q1, Q3
2- K+Na-HCO_3: Q5, Q11
3- K+Na-HCO_3, SO_4: Q2, Q4, Q6, Q8, Q10, Q12
4- K+Na-SO_4: Q7, Q13, Q14, Q15
5- K+Na-Cl: Q9, Q16, Q17, Q18, W
6- Mg-Cl: S

The water resources of the south of the ophiolitic outcrop have chloride water type (Fig. 7).

According to Stiff diagrams, as the water samples evolve from the Ca, K, Na-HCO_3 facies to the K, Na, Mg-Cl facies, the total dissolved ions (TDI) values increase concurrently. The changes in total dissolved solids (TDS) values according to the type and facies of water samples do not show a clear trend. Therefore, it is better to rely on TDI than on TDS. Sodium facies are the dominant groundwater facies in the study area. Therefore, the process of hydrogeochemical evolution in the Naeen aquifer is as follows: HCO_3 → HCO_3 (SO_4) → SO_4 (HCO_3) → SO_4 → SO_4 (Cl) → Cl. Considering the direction of groundwater flow in the aquifer, water samples change from Ca, K, Na-HCO_3 type in the west of the area to K, Na-Cl type in the east of the study area.

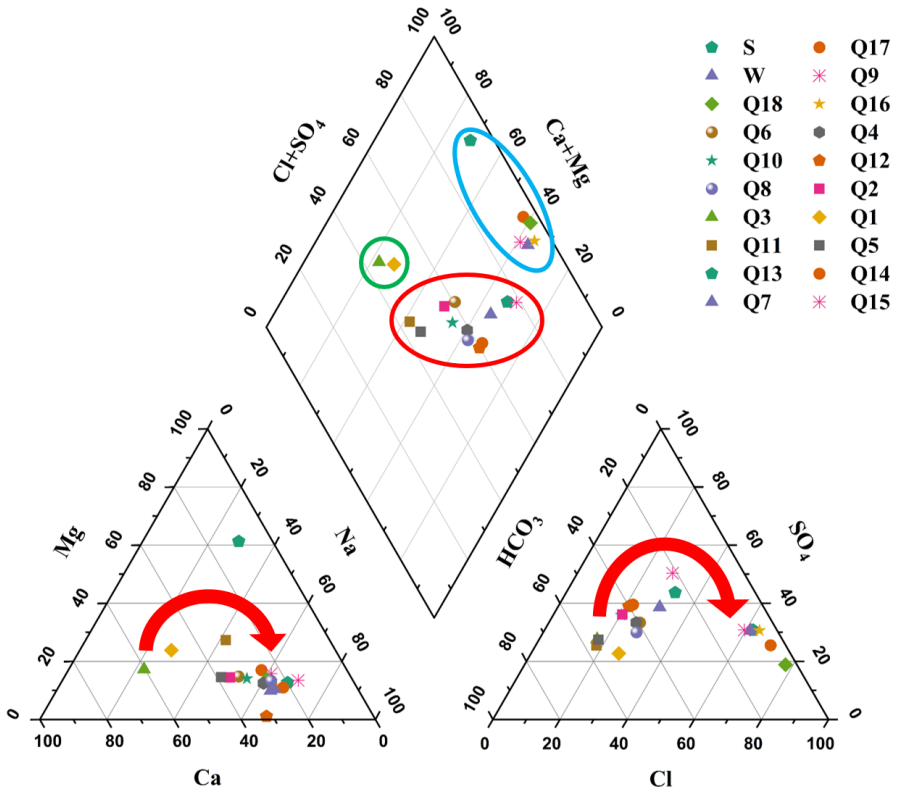

Fig. 6 - Location of the Naeen groundwater samples in the Piper diagram. The reader is referred to the PDF online for a colour version.

Scholler diagram. According to the Scholler diagram, groundwater samples in the west and southwest of the study area are within the permissible range for all parameters (Fig. 8). In contrast, the ion concentrations of samples of W, Q18, Q17, and Q16, especially for sulfate, sodium, and magnesium, are higher than the permissible limits for drinking purposes. These four samples are located in the area of Naeen City and in the vicinity of ophiolitic outcrops. The permissible and non-permissible values of the main ions in the Scholler diagram are considered based on the WHO standards (World Health Organization, 2022).

Wilcox diagram. According to the results of the Wilcox diagram, the groundwater samples of the Naeen aquifer are divided into five categories (Fig. 9). In particular, among the four samples that are located in the vicinity of the ophiolitic outcrops, the samples from Q17, Q16, and W are in the C4S4 category and are not suitable for agriculture, whereas sample Q18 is not included in the Wilcox plot due to its very high EC value.

Bivariate graphs. In the bivariate graphs of TDI against the main ions of the water resources of the study area (Fig. 1S), a TDI value equal to 100 mEq l^{-1} represents the boundary between the low-TDI southern and western samples and the eastern groundwater samples adjacent to the ophiolitic rocks. The five samples with TDI > 100 mEq l^{-1} show a concurrent increase in the concentrations of Cl, SO_4, Na, Mg, and Ca ions, as well as in TDI, and are positioned (apart from the Q18 sample in the SO_4 vs. TDI plot, see below) along a trend passing through the origin of the axes, which is representative of pure water vapour. Thus, the sample points move progressively away from the origin due to increasing evaporation, which is the simplest process possibly controlling their characteristics. The decreasing HCO_3 concentration with increasing TDI of the samples of Q9, W, Q16, and Q17 might be due to calcite precipitation, which is expected to have negligible effects on Ca concentration since the latter is much higher than the HCO_3 concentration. The position of the Q18 sample below the evaporation line in the SO_4 vs. TDI graph cannot be explained by gypsum precipitation because all the considered aqueous solutions are undersaturated with respect to this mineral. Considering that the Q18 sample is found above the alignment of the samples with TDI > 100 mEq l^{-1} in the HCO_3 vs. TDI graph, it might be affected by bacterial sulfate reduction sustained by concurrent oxidation of organic matter [CH_2O], as indicated by the following reaction (Berner and Berner, 1996; Stumm and Morgan, 1996):

$$SO_4^{2-} + 2\ CH_2O = 2\ HCO_3^- + H_2S.$$

The combined diagram of Mg^{2+}/Ca^{2+} versus Na^+/Ca^{2+} shows the lithological units affecting water quality (Han and Liu, 2003). According to this diagram (Fig. 10), the quality of groundwater resources of the Naeen aquifer is mainly controlled by silicate dissolution and subordinately by carbonate dissolution. Moreover, evaporite dissolution cannot be disregarded because (1) gypsum is present in the Qom formation (thick successions of marine marls, limestones, gypsum and siliciclastics; Reuter et al. 2009) cropping out in the study area, and (2) the minerals typical of evaporite deposits, such as halite and gypsum, may be locally deposited upon extreme evaporation and may be redissolved, although to a local scale only.

Definite ionic ratios

The source rock minerals of aquifers can be identified from the composition of the groundwater and the concentration of each of the ions. If the composition of an aquifer is known, the process of investigating the hydrogeochemical data for possible reactions in the groundwater will be easy. The ion ratios used for the groundwater samples of the Naeen aquifer are based on the mass balance method (Table 3).

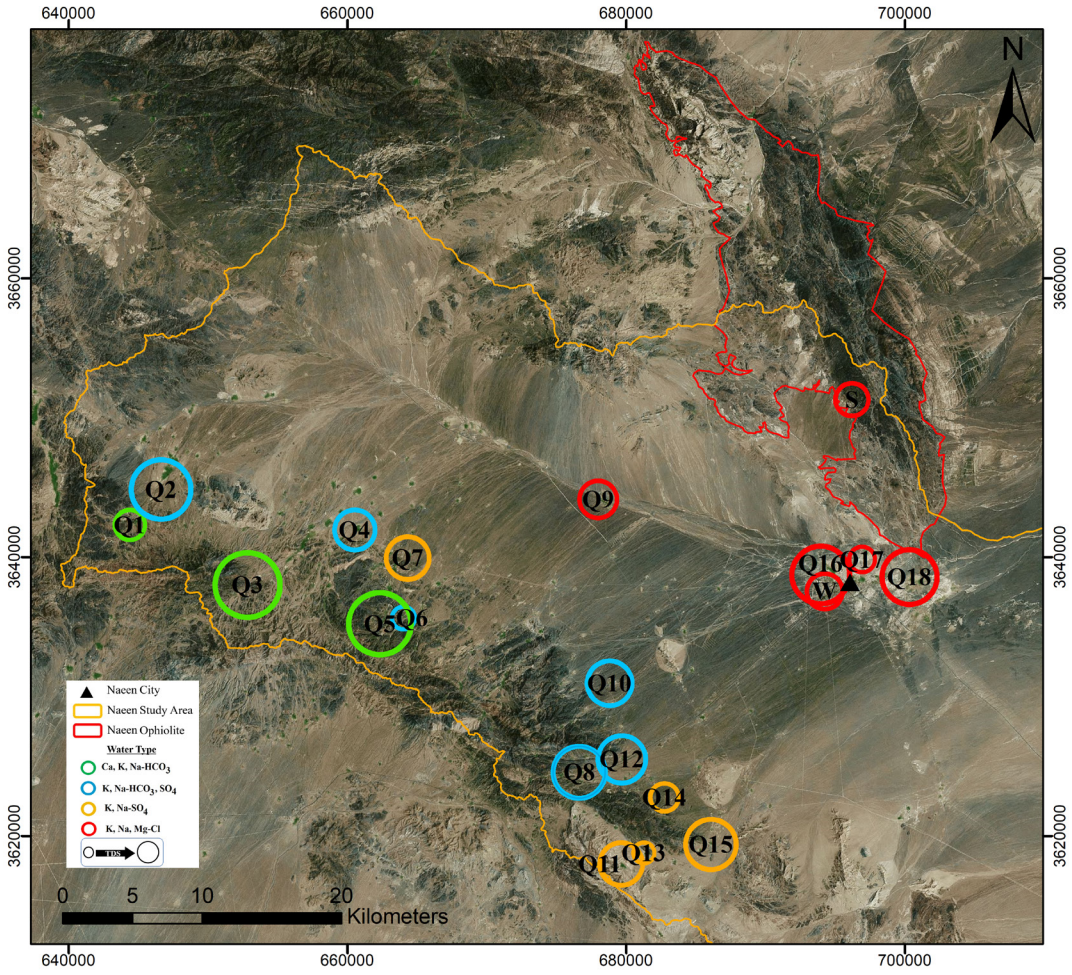

Fig. 7 - Location of the Naeen groundwater samples showing the chemical type and the TDI values. The reader is referred to the PDF online for a colour version.

Table 3 - Source-rock deduction in the Naeen groundwater [uncertainty 0.1, reference values from WATEVAL (Hounslow, 1995).

Samples	Na/Na + Cl> 0.5	Mg/Ca+ Mg < 0.5	Ca/Ca+SO_4 > 0.5	0.8 < Ca + Mg/SO_4 < 1.2	Cl/ ΣAnions < 0.8
W	0.51	0.27	0.46	1.18	0.62
S	0.32	0.86	0.25	2.36	0.62
Q6	0.66	0.31	0.50	1.44	0.27
Q7	0.68	0.30	0.39	0.91	0.30
Q17	0.45	0.40	0.50	1.66	0.70
Q1	0.51	0.33	0.68	3.20	0.26
Q12	0.76	0.03	0.45	0.84	0.21
Q11	0.70	0.47	0.55	2.29	0.18
Q18	0.44	0.35	0.57	2.08	0.78
Q14	0.75	0.33	0.36	0.83	0.22
Q13	0.68	0.39	0.31	0.74	0.32
Q9	0.51	0.41	0.43	1.26	0.59
Q15	0.71	0.45	0.24	0.59	0.28
Q4	0.70	0.32	0.45	1.19	0.26
Q8	0.69	0.35	0.45	1.26	0.28
Q2	0.71	0.29	0.50	1.40	0.20
Q16	0.50	0.31	0.44	1.14	0.64
Q10	0.73	0.31	0.47	1.26	0.20
Q5	0.73	0.27	0.59	1.94	0.18
Q3	0.57	0.22	0.69	2.81	0.17

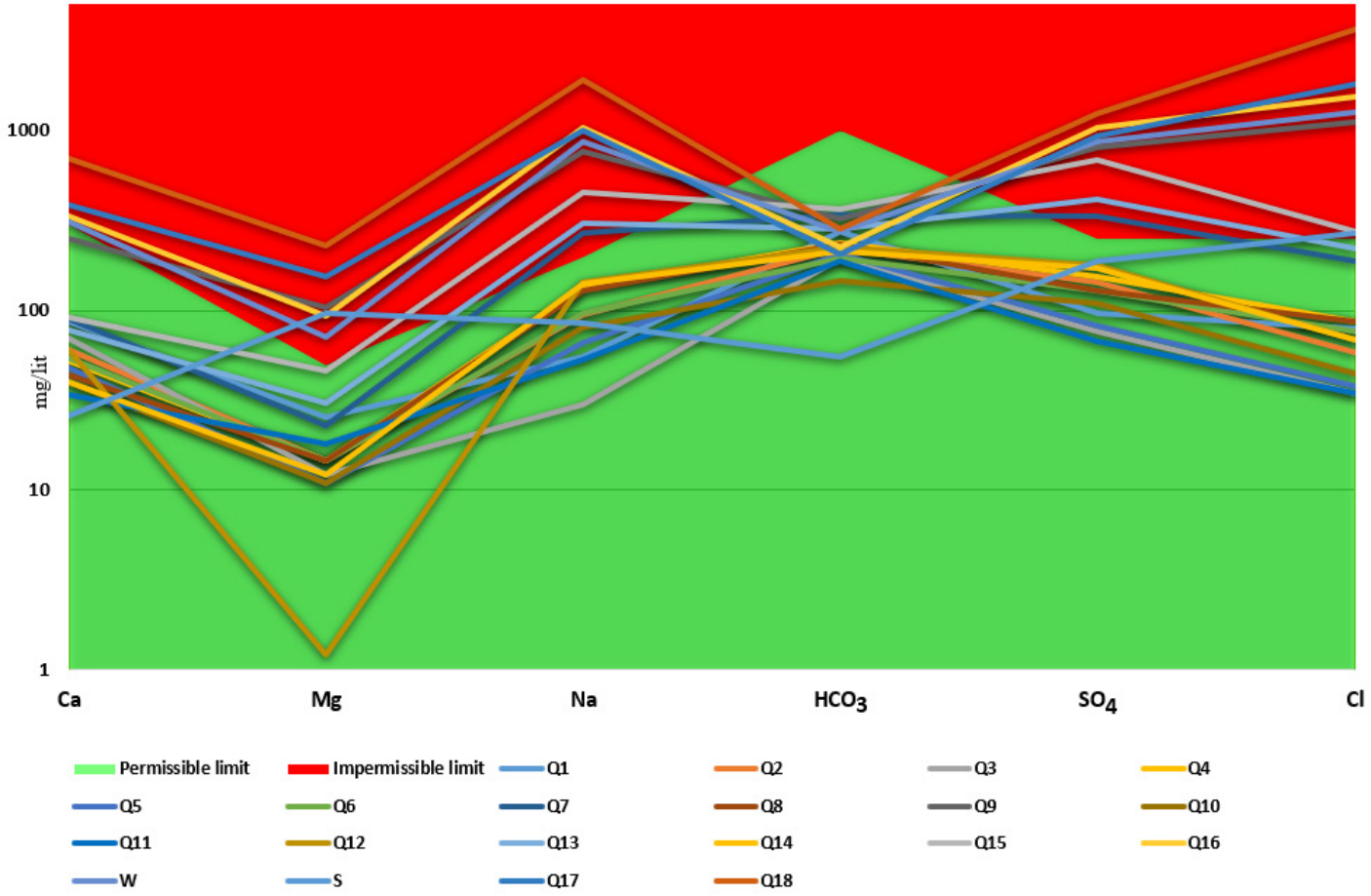

Fig. 8 - Location of the Naeen groundwater samples in the Scholler diagram. The reader is referred to the PDF online for a colour version.

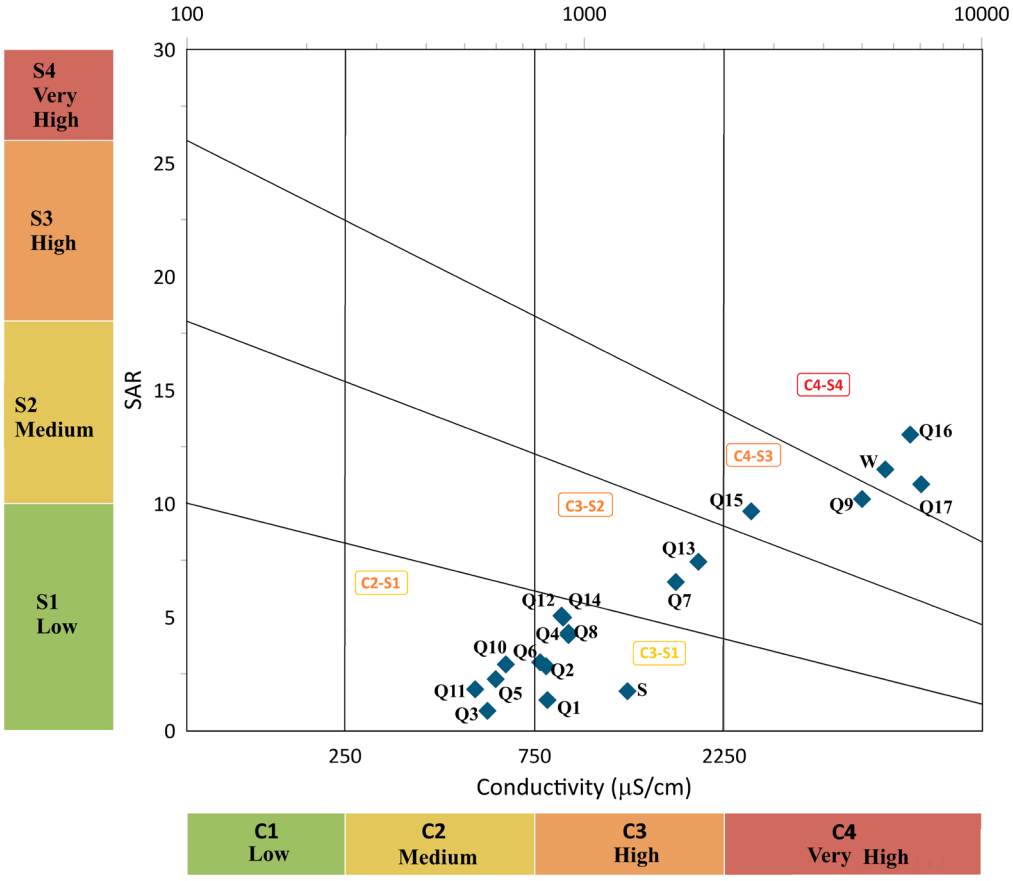

Fig. 9 - Location of the Naeen groundwater samples in the Wilcox diagram.

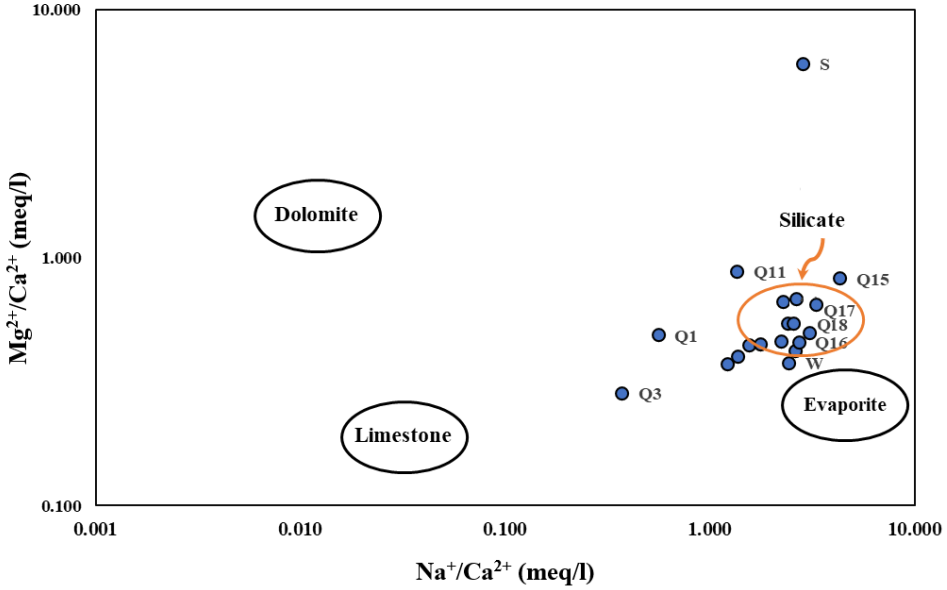

Fig. 10 - The position of the Naeen groundwater samples in the Mg^{2+}/Ca^{2+} versus Na^{+}/Ca^{2+} diagram (based on Gaillardet et al., 1999).

The ratio of $\frac{Na^+}{Na^+ + Cl^-}$ in almost all the water samples is more than 0.5, indicating that sodium enters the groundwater from a source other than the dissolution of halite, such as the weathering of plagioclases (albite). For the water sample S (i.e., of spring located in the area where ophiolitic rocks crop out), due to the high concentration of chloride (7.9 meq/L) compared to sodium (3.7 meq/L), this value is less than 0.5. In most samples, the ratio of $\frac{Ca^{2+}}{Ca^{2+} + SO_4^{2-}}$ is around 0.5, which indicates the possible origin of calcium from carbonate or silicate dissolution. Values less than 0.5 for this ratio in some samples are due to the high concentration of SO4 compared to the concentration of Ca ions. The reduction of Ca ion concentration in groundwater might occur as a result of the ion exchange process or calcite precipitation. Values of the ratio $\frac{Ca^{2+} + Mg^{2+}}{SO_4^{2-}}$, which are greater than 0.8 and lower than 1.2, might indicate the occurrence of dedolomitization, that is, precipitation of calcite and dissolution of dolomite triggered by gypsum/anhydrite dissolution (Hounslow, 1995). Based on the values of the $(Ca + Mg)/SO_4$ ratio, this process might occur in almost half of the water samples in the study area.

In all investigated samples, the ratio of $\frac{Mg^{2+}}{Ca^{2+} + Mg^{2+}}$ is less than 0.5, which indicates the possible dissolution of both calcite and dolomite in the study area. The exception in this case is the water of the spring located in the ophiolitic mass, where this ratio is 0.86 due to the high concentration of Mg. The weathering of Mg-silicates in ultramafic rocks such as serpentinite increases the concentration of Mg compared to Ca in groundwater (Hounslow, 1995). Values of the ratio $\frac{Cl^-}{\Sigma Anion}$ lower than 0.8 might indicate rock weathering. According to the calculated specific ratios, the dissolution of carbonate and silicate minerals might impact the hydrogeochemical conditions in the Naeen aquifer. However, dissolution of a given mineral can occur only if the aqueous solution is undersaturated with respect to it. For this reason, it is important to compute the saturation state of the waters of interest concerning relevant minerals, which is investigated in the next section.

Saturation profiles

Based on the saturation index calculated through hydrogeochemical modeling for the Naeen groundwater samples, all samples are undersaturated with gypsum and halite and supersaturated with calcite and dolomite, apart from a few exceptions (Fig. 11). This means that dissolution of halite and gypsum (which is actually present in interlayers of the Qom formation cropping out in the study area) is possible. In contrast, the dissolution of calcite and dolomite is impossible in general, whereas the precipitation of these two carbonate minerals is possible. This does not exclude the occurrence of calcite and dolomite dissolution in an early stage of evolution when the waters were possibly undersaturated with these two carbonate solid phases.

Thus, it cannot be excluded that the dominant process occurring in the aquifer, upstream of the sampling points, is carbonate dissolution. The quality of the groundwater in these sites, upstream of the sampling points, is controlled by calcite and dolomite dissolution, whereas gypsum dissolution might have a partial and local effect. As discussed in the previous section, gypsum/anhydrite dissolution might cause dedolomitization, that is, precipitation of calcite and dissolution of dolomite (Hounslow, 1995).

When groundwater resources saturated or supersaturated with carbonate minerals interact with igneous rocks containing sodium plagioclase, the dissolution of this silicate driven by conversion of CO_2 to bicarbonate is possible. The process causes an increase in both bicarbonate and sodium as well as the possible acquisition of the sodium-bicarbonate composition. Nevertheless, sodium-bicarbonate composition might also be acquired through cation exchange. A typical example is freshening, which is the backflow of calcium-bicarbonate waters in coastal areas previously affected by salinization.

Hierarchical cluster analysis

Based on the Pearson correlation matrix for the main ions of the Naeen aquifer water samples (Fig. 12), all the investigated variables, except for bicarbonate, have a high correlation with each other, and there is no significant negative correlation observed among the available variables. This finding was predictable because correlation coefficients are mainly

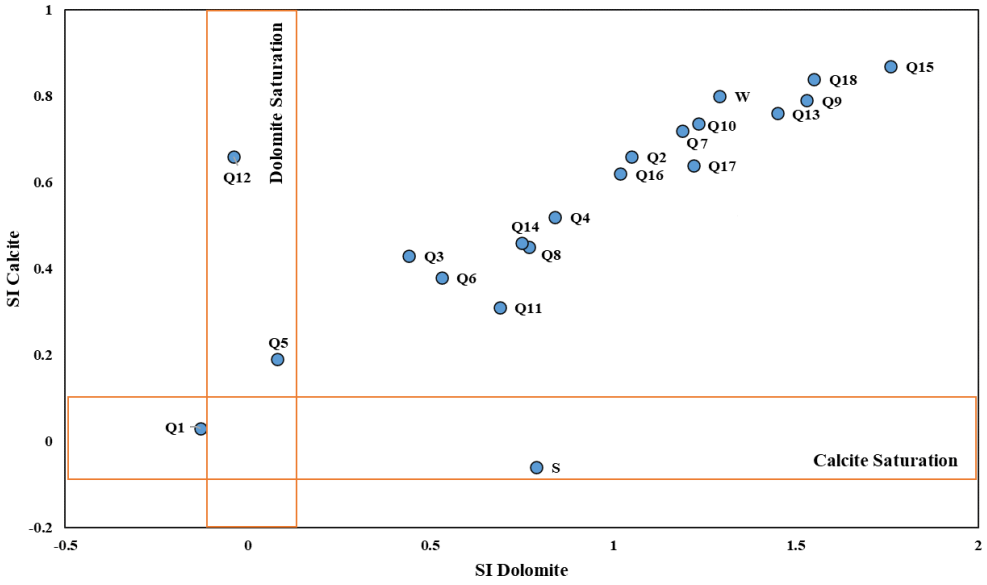

Fig. 11 - Calcite and dolomite saturation indices in the Naeen aquifer.

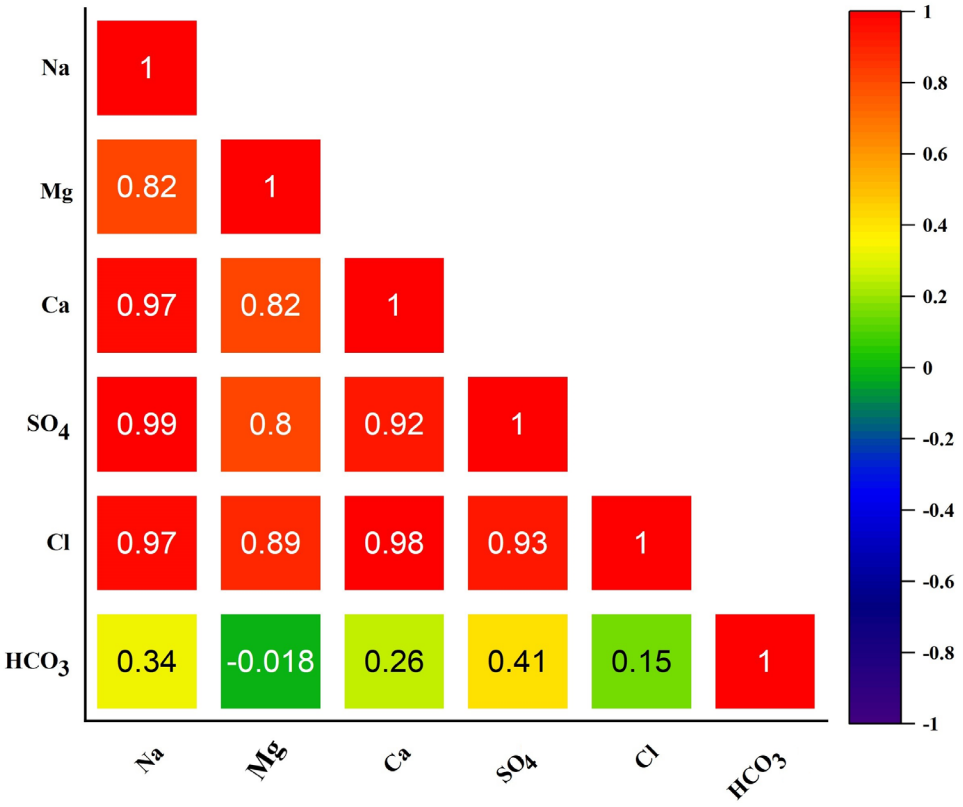

Fig. 12 - Pearson correlation matrix for the Naeen groundwater samples.

affected by the samples of high salinity, which have high concentrations of Cl, SO_4, Na, Ca, and Mg.

For the hydrogeochemical classification of the groundwater samples of the study area, the Q-Mode and R-Mode hierarchical clustering methods were used in separate exercises. The average Euclidean distance method was used to calculate the similarity coefficient in quantitative traits. The grouping of water samples was done according to Ward Jr. (1963). In this method, in each step of the analysis, the combination of each pair of samples may be taken into consideration, and both groups whose integration increases the amount of variance to a lesser extent are placed in one group, and the same is also followed in the next stages of grouping.

Hierarchical Q-Mode cluster analysis was performed based on the values of hydrogeochemical parameters including EC, Na, K, Ca, Mg, Cl, SO_4, and HCO_3 (Fig. 13). Based on this analysis, the groundwater samples of the Naeen aquifer are classified into two main groups: chloride and bicarbonate-sulfate. The samples located in the south of the ophiolitic mass (Q17, Q9, Q18, Q16, S, and W) with high TDI values and chloride type are placed in one group. Due to EC and TDI values that are much higher than other samples, Q18 is placed in a separate group, while its chemical properties are similar to other samples located in the south of the ophiolitic mass, and together with them, it is considered a subgroup of one main group.

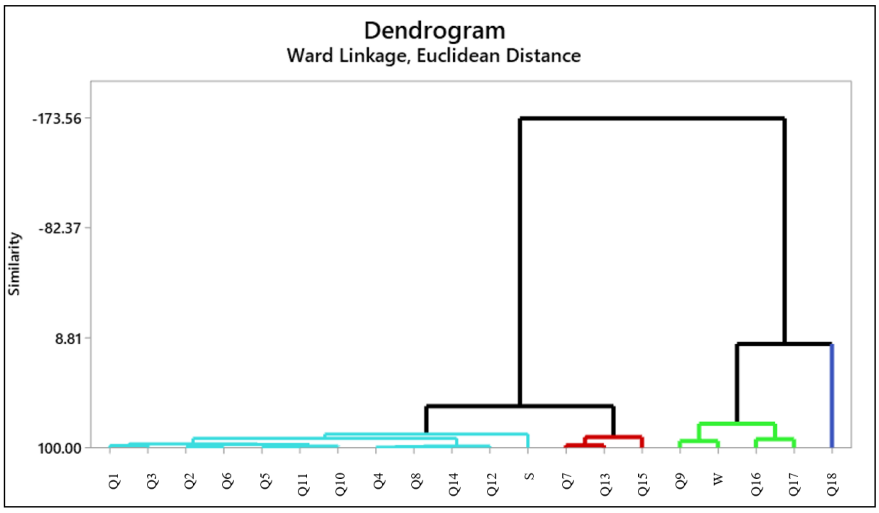

Fig. 13 - Q-Mode cluster analysis for the Naeen groundwater samples.

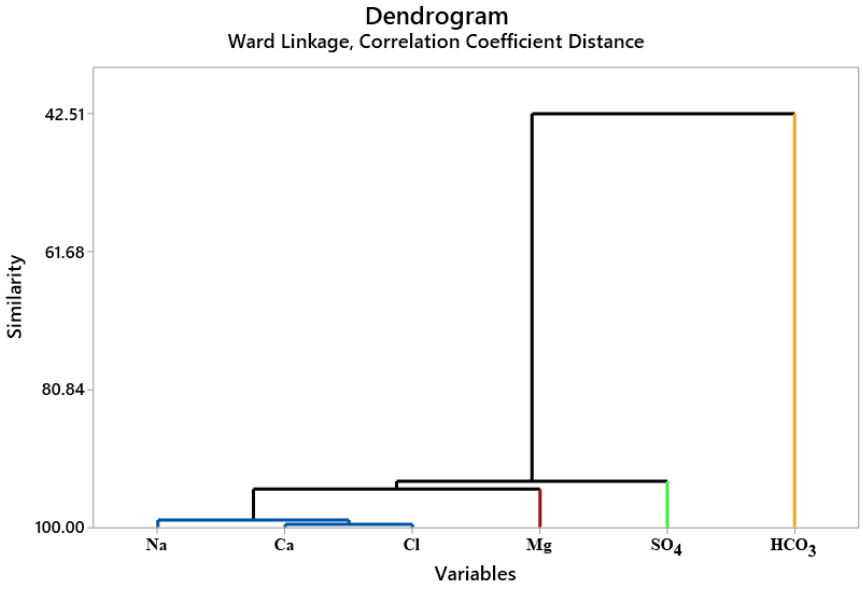

Fig. 14 - R-Mode cluster analysis for the groundwater samples of the Naeen aquifer.

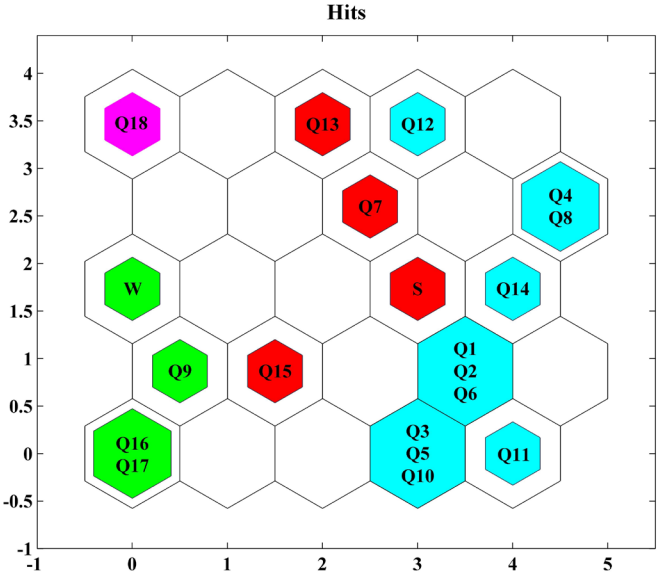

Fig. 15 - Output groups based on the self-organizing map of study samples.

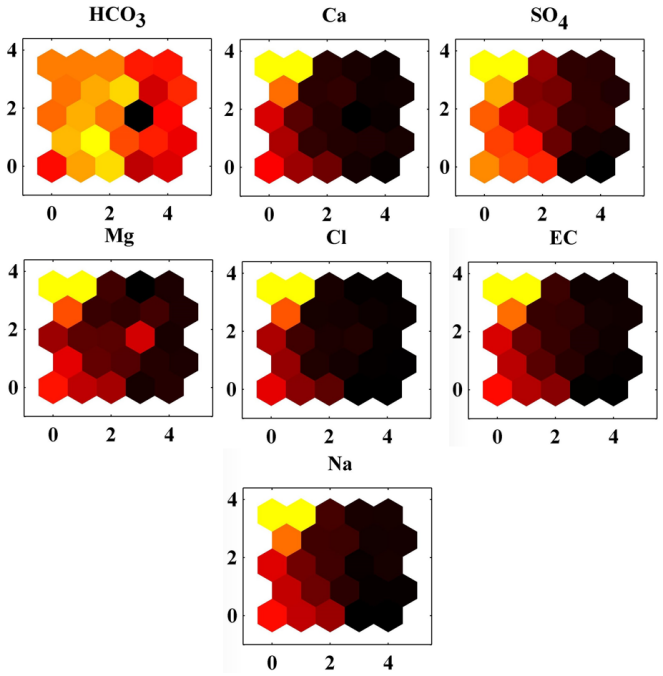

Fig. 16 - Effects of input variables on each node for Naeen groundwater samples.

Other samples are a mixture of bicarbonate, bicarbonate-sulfate, and sulfate samples, whose lack of full hydrochemical maturity has caused them to find conditions close to each other in the hierarchical clustering process. The water group, which contains the largest number of water samples, is considered an elementary member with the dominant type of bicarbonate and low TDI values. The Q18 sample is introduced as the final member in the path of hydrochemical evolution of the Naeen aquifer. Other samples show mixing between the first and last groups.

Based on the hierarchical cluster analysis of samples (R-Mode) for the water samples of the study area, calcium and chloride are the most similar to each other, having a very high correlation coefficient (Fig. 14). Other main ions are placed in separate groups.

Self-organizing maps

Based on the output of the self-organizing maps (SOMs) for the Naeen groundwater, samples Q9, W, Q16, and Q17, located in the south of the ophiolitic mass, are placed in one group (Fig. 15), whereas sample Q18 is attributed to a separate group due to its TDI higher than that of samples Q9, W, Q16 and Q17. According to the Stiff and Piper diagrams, all these samples have high TDI values and belong to the sodium-chloride type. Samples S, Q13, Q15, and Q7 are placed in the same group in SOM, although sulfate is the prevailing anion in sa les, with bicarbonate to bicarbonate-sulfate chemistry and almost similar TDI values, are in another group.

Fig. 16 shows the effect of input variables on each node in SOMs. In these maps, the lighter the colour of the node, the more impact the parameter has on that node. In fact, the sample corresponding to that node has the highest concentration or value of that parameter. SOM is useful for detecting the maximum and minimum concentration in the shortest time for a large amount of data. The output of these maps for specific groundwater samples shows that all samples have similar bicarbonate concentrations. On the other hand, almost all the other parameters have higher values in the samples of the left side of SOM, that is, in the group of high-TDI chloride waters.

Investigating the effect of ophiolitic mass on groundwater salinity

The overall evaluation of groundwater quality in terms of salinity is usually performed based on TDS. Various classifications have been presented for TDS, and in most of them, the limits are determined based on drinking water. According to the classifications of Todd and Mays (2005) and Freeze and Cherry (1979), fresh waters are waters with TDS less than 1000 mg l^{-1}, whereas waters with TDS values greater than 1000 mg l^{-1} are considered saline waters. Accordingly, 40% of the groundwater samples of the Naeen aquifer are in the range of saline water. Generally, salinity is determined by increasing chloride concentration. Chloride is a conservative constituent and its concentration changes can be completely related to the input source.

Chloride concentration in groundwater samples of the Naeen aquifer changes in the range of 35-3800 mg l^{-1} and increases from the southwest to the east where ophiolitic rocks crop out (Fig. 2S). The high correlation (> 0.8) of chloride ion with all the main ions (except bicarbonate) and also with the EC parameter suggests that the main factor controlling the quality changes of the groundwater of the Naeen aquifer is evaporation (Fig. 3S).

Naeen aquifer is mainly recharged by the mountainous reliefs located to the west of the plain, where carbonate, igneous, and metamorphic formations crop out, and subordinately by the mountainous reliefs positioned to the east-northeast of the plain, where the ophiolitic complexes crop out. The quality of Naeen groundwater is affected by water-rock interactions including cation exchange, dissolution- precipitation of carbonates including calcite and dolomite, and to some extent, dissolution of gypsum. There are no clear outcrops of evaporite formations in the study area and the only available evaporite deposits are gypsum interlayers of the Qom Formation, which cannot have a significant effect on the hydrogeochemical characteristics of groundwater. In addition, subsurface studies and well logs of selected piezometric wells in Naeen alluvial formations have not confirmed the existence of any subsurface evaporite layer and show alluvial formations constituted only by clay, sand, and gravel.

The abundance of fine-grained deposits such as clay and marl deposits and the relatively low values of hydraulic conductivity in the Naeen aquifer increase both the groundwater residence time in the aquifer and the hydrological response time to recharge waters, which is more than six months based on the representative hydrograph of the aquifer. As a result, the speed and intensity of the water-rock interactions in the aquifer increase, resulting in an increase in the solutes and salinity of the groundwater. Furthermore, the main process driving the increase in salinity is evaporation.

The Naeen ophiolitic complex extends northeastwards, from the north of Naeen city, in the Daghe Sorkh basin. The EC values of the groundwater samples from the Daghe Sorkh area, located to the west of the ophiolite outcrop, are far higher than the values of this parameter in the Naeen aquifer, with values up to 30,000 microS/cm, which is twice as high as the maximum EC value in the Naeen aquifer (Fig. 17). The highest salinity of the groundwater in the Daghe Sorkh belongs to the Sohail well and Separo Qanat, located close to the mountainous reliefs where the ophiolitic rocks crop out, with EC values of 30,000 and 15,000 microS/cm and chloride concentrations of 275 and 120 mEq l^{-1}.

According to the graphs of major ions versus EC for the groundwater samples of the Naeen and Daghe Sorkh aquifers (Fig. 18), the similar distribution of the water samples of both areas indicates the similarity of the processes controlling the chemistry of these samples.

CONCLUSIONS

The present study is an attempt to investigate the groundwater quantity and quality in the Naeen aquifer using graphical, statistical, and hydrogeochemical methods. The hydrograph of the aquifer shows that in the last 16 years, the groundwater level of the Naeen aquifer has dropped by about 2 m, and the changes in precipitation in the study area are one of the controlling factor. The Naeen aquifer is mainly recharged by the mountainous reliefs located to the west of the plain, where carbonate, igneous, and metamorphic formations crop out, and subordinately by the mountainous reliefs positioned to the east-northeast of the plain, where the ophiolitic complexes crop out. Based on the Piper and Stiff diagrams, the groundwater samples of the Naeen aquifer can be divided into three main groups: Ca, K, Na-HCO_3, K, Na-SO_4, and K, Na, Mg-Cl. The results of the qualitative evaluation of the aquifer indicate relatively alkaline conditions with EC values in the range of 530-12700 microS/cm. According to the Scholler diagram, the samples located close to Naeen

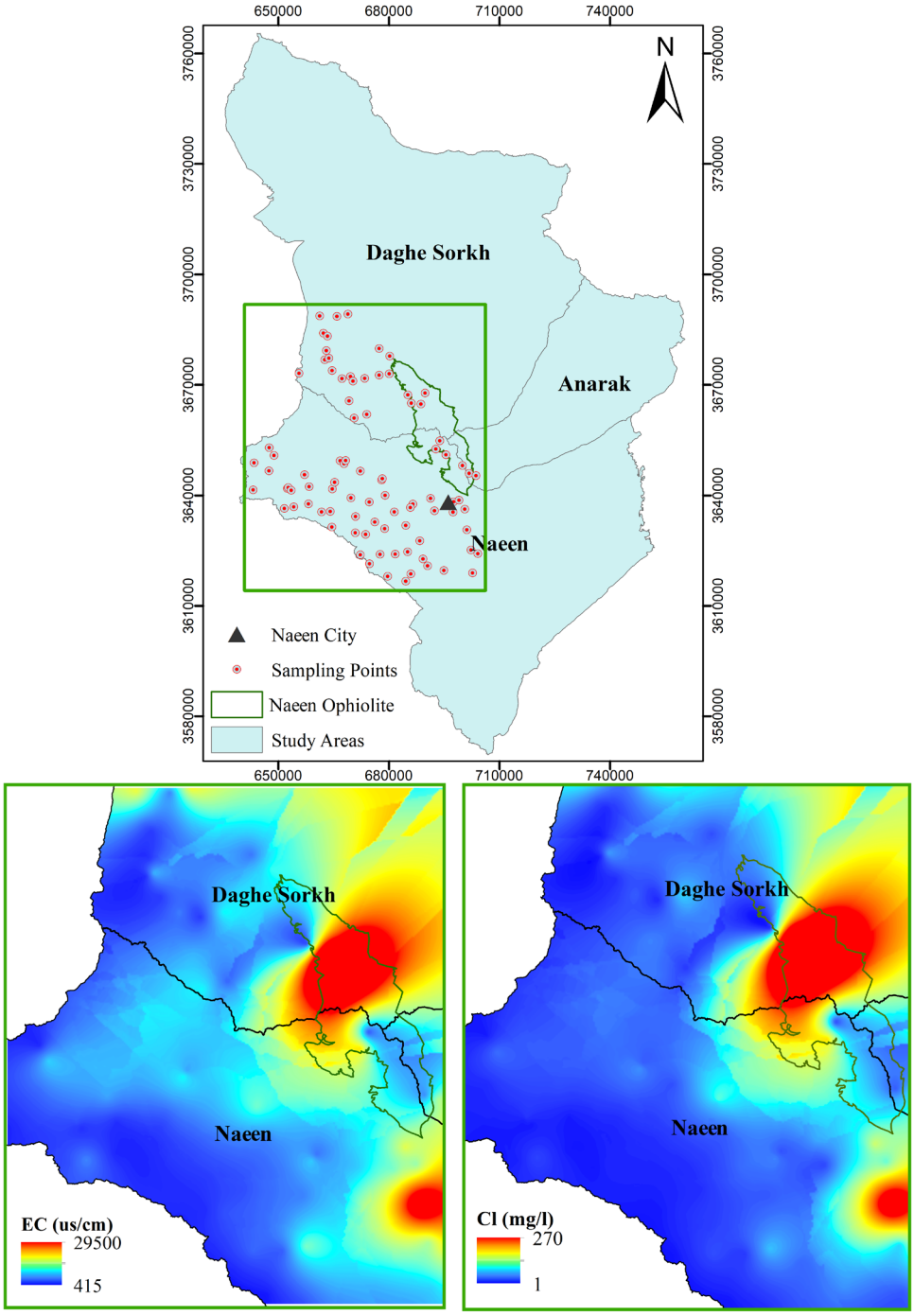

Fig. 17 - Changes of Cl ion (right side) and EC values (left side) in the groundwater of the Daghe Sorkh and Naeen areas. The reader is referred to the PDF online for a colour version.

City and in the vicinity of the ophiolite outcrop have concentrations of sulfate, sodium, and magnesium higher than the permissible limits of drinking water.

According to the results of the Wilcox diagram, in this part of the aquifer, the groundwater samples are not suitable for agriculture. Based on the saturation indices calculated through hydrogeochemical modeling, the groundwaters of interest are saturated or supersaturated with calcite and dolomite. Hierarchical cluster analysis of R-Mode and Q-Mode for the groundwater samples of the Naeen aquifer shows that the samples are generally placed in two main groups of K, Na, Mg-Cl (samples located to the south of the mountainous reliefs where ophiolitic rocks crop out) and Ca, K, Na-HCO_3, SO_4. According to SOMs, the Naeen aquifer groundwater samples are found in three groups: the group with high TDI values and K, Na, Mg-Cl type (near the ophiolitic mass), the group with medium TDI values and K, Na-SO_4 type, and the group with low TDI values encompassing Ca, K, Na-HCO_3 type to Ca, K, Na-HCO_3, SO_4 type.

Analysis of qualitative data shows that the processes of cation exchange, dissolution of carbonates, and weathering of silicates are the dominant processes affecting the chemical quality of groundwater in the region. In addition, the fineness of aquifer sediments and consequently, the increase in residence time, the large amount of evaporation compared to the rainfall in the area, and the return of agricultural water with very high salinity, have also caused an increase in the EC of groundwater in the study area.

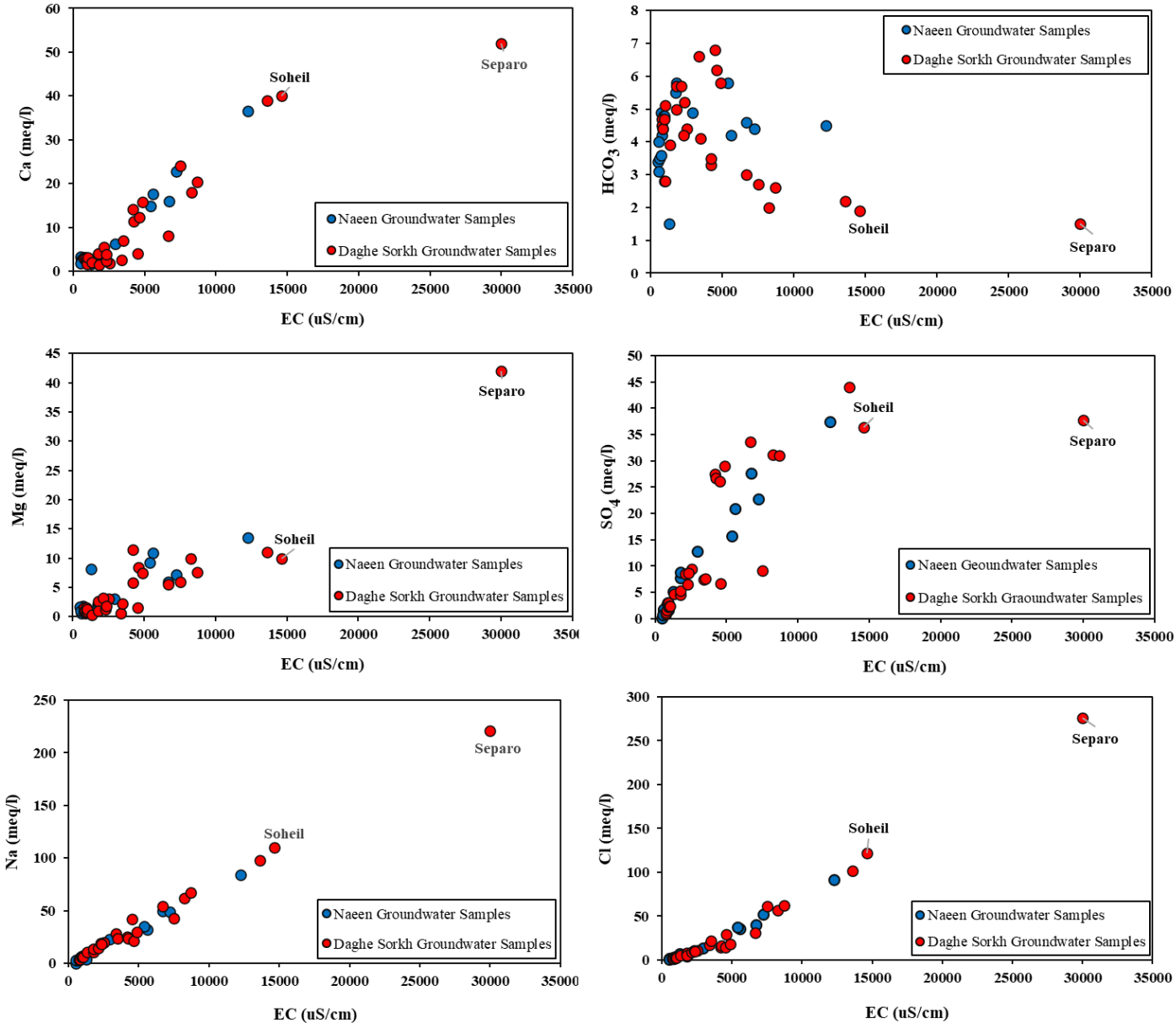

Fig. 18 - Graphs of major ions versus EC for water samples of the Naeen and Daghe Sorkh. The reader is referred to the PDF online for a colour version.

Supplementary Material

Supplementary data associated with this article can be found in the online version at https://ofioliti.it/index.php/ofioliti/article/view/719

REFERENCES

Aghanabati A., 2004. Geology of Iran. Geological Survey of Iran Publications, Tehran, 640 pp.

Alai S. and Foudazi M., 2004. Geological map of Naeen (1:100000). Geological Survey of Iran.

Apollaro C., Fuoco I., Brozzo G. and De Rosa R., 2019. Release and fate of Cr (VI) in the ophiolitic aquifers of Italy: The role of Fe (III) as a potential oxidant of Cr (III) supported by reaction path modelling. Sci. Tot. Environ, 6 60: 1459-1471. https://doi.org/10.1016/j.scitotenv.2019.01.103.

Apollaro C., Marini L., Critelli T., Barca D., Bloise A., De Rosa R., Liberi F. and Miriello D., 2011. Investigation of rock-to-water release and fate of major, minor, and trace elements in the metabasalt-serpentinite shallow aquifer of Mt. Reventino (CZ, Italy) by reaction path modeling. Appl. Geochem., 26: 1722-1740. https://doi.org/10.1016/j.apgeochem.2011.04.028.

APHA, 2017. Standard Methods for the Examination of Water and Wastewater. American Public Health Association, 21 Ed., American Water Works Association (AWWA) and Water Environment Federation (WEF), 1796 pp.

Ball J.W. and Izbicki J.A., 2004. Occurrence of hexavalent chromium in ground water in the western Mojave Desert, California. Appl. Geochem., 19: 1123–1135. https://doi.org/10.1016/j.apgeochem.2004.01.011.

Berner E.K. and Berner R.A., 1996. Global environment: water, air and geochemical cycles. Prentice Hall, 464 pp.

Bertolo R., Bourotte C., Hirata R., Marcolan L. and Sracek O., 2011a. Geochemistry of natural chromium occurrence in a sandstone aquifer in Bauru Basin, São Paulo State, Brazil. Appl. Geochem., 26: 1353-1363. https://doi.org/10.1016/j.apgeochem.2011.05.009.

Bertolo R., Bourotte C., Marcolan L., Oliveira S. and Hirata R., 2011b. Anomalous content of chromium in a Cretaceous sandstone aquifer of the Bauru Basin, state of São Paulo, Brazil. J. South Am. Earth Sci., 31: 69-80. https://doi.org/10.1016/j.jsames.2010.10.002.

Boschetti T. and Toscani L., 2008. Springs and streams of the Taro-Ceno Valleys (Northern Apennine, Italy): reaction path modeling of waters interacting with serpentinized ultramafic rocks. Chem. Geol., 257 (1-2): 76-91. https://doi.org/10.1016/j.chemgeo.2008.08.017.

Bruni J., Canepa M., Chiodini G., Cioni R., Cipolli F., Longinelli A. and Zuccolini M.V., 2002. Irreversible water-rock mass transfer accompanying the generation of the neutral, Mg–HCO_3 and high-pH, Ca-OH spring waters of the Genova province, Italy. Appl. Geochem., 17 (4): 455-474. https://doi.org/10.1016/S0883-2927(01)00113-5.

Critelli T., Vespasiano G., Apollaro C., Muto F., Marini L. and De Rosa R., 2015. Hydrogeochemical study of an ophiolitic aquifer: a case study of Lago (Southern Italy, Calabria). Environ. Earth Sci., 74: 533-543. https://doi.org/10.1007/s12665-015-4061-z.

Dermatas D., Mpouras T., Chrysochoou M., Panagiotakis I., Vatseris C., Linardos N., Theologou E., Boboti N., Xenidis A., Papassiopi N. and Sakellariou L., 2015. Origin and concentration profile of chromium in a Greek aquifer. J. Hazard. Mater., 281: 35-46. https://doi.org/10.1016/j.jhazmat.2014.09.050.

Dewey J.F. and Bird J M., 1971. Origin and emplacement of the ophiolite suite: Appalachian ophiolites in Newfoundland. J. Geophys, Res., 76 (14): 3179-3206.

Dilek Y. and Furnes H., 2014. Ophiolites and Their Origins. Elements. 10: 93-100. https://doi.org/10.2113/GSELEMENTS.10.2.93.

Dokou Z., Karagiorgi V., Karatzas G.P., Nikolaidis N.P. and Kalogerakis N., 2016. Large scale groundwater flow and hexavalent chromium transport modeling under current and future climatic conditions: the case of Asopos River Basin. Environ. Sci. Pollut. Res., 23 (6): 5307-5321. https://doi.org/10.1007/s11356-015-5771-1.

Fantoni D., Bronzzo G., Canepa M., Cipoli F., Marini L., Ottonello G. and Zuccolini N.V., 2002. Natural hexavalent Chromium in groundwater interacting with ophiolittic rocks. Environ. Geol., 42: 871-882. https://doi.org/10.1007/s00254-002-0605-0.

Fazlnia A.N., Kodadady F. and Pirkharati H., 2012. Hydrogeochemical evaluation of groundwater sources in the ophiolitic regions of north-northwest of Khoy and Qara Ziauddin to identify water quality and determine environmental effects. J. new Findings Applied Geol., 6 (11): 46-70.

Freeze A.R. and Cherrey J.A., 1979. Groundwater. Prentice-Hall, 624 pp.

Gaillardet J., Dupre B., Louvat P. and Allègre C.J., 1999. Global silicate weathering and CO_2 consumption rates deduced from the chemistry of large rivers. Chem. Geol., 159 (1–4): 3-30. https://doi.org/10.1016/S0009-2541(99)00031-5.

Gonzalez A.R., Ndung'u K. and Flegal A.R., 2005. Natural occurrence of hexavalent chromium in the Aromas Red Sands Aquifer California. Environ. Sci. Technol., 39: 5505-5511. https://doi.org/10.1021/es048835n.

Gray D.J., 2003. Naturally occurring Cr^{+6} in shallow groundwaters of the Yilgarn Craton, Western Australia. Geochem.- Explor. Environ. A., 3: 359-368. https://doi.org/10.1144/1467-7873/03-012.

Güler C., Thyne G.D., Tala H. and Yjldjrjm Ü., 2017. Processes governing alkaline groundwater chemistry within a fractured rock (Ophiolitic mélange) aquifer underlying a seasonally inhabited headwater area in the Aladallar range (Adana, Turkey). Geofluids, 2: 1-21.

Hajizadeh Namaghi H., Karami Gh.H. and Saad S., 2011. A study on chemical properties of groundwater and soil in ophiolitic rocks in Firuzabad, east of Shahrood, Iran: with emphasis to heavy metal contamination. Environmental Monitoring and Assessment, 174: 573-583. https://doi.org/10.1007/s10661-010-1479-3.

Hall R., 1976. Ophiolite emplacement and the evolution of the Taurus suture zone, southeastern Turkey. Geol. Soc. Am. Bull., 87 (7): 1078-1088.

Hamilton W., 1969. Mesozoic California and the underflow of Pacific mantle. Geol. Soc. Am. Bull., 80 (12): 2409-2430. https://doi.org/10.1130/0016-7606(1969)80[2409:MCATUO]2.0.CO;2.

Han G. and Liu C., 2003. Water geochemistry controlled by carbonate dissolution: a study of the river water draining Karst-dominated terrain, Guizhou Province, China. Chem. Geol., 204 (1-2): 1-21. https://doi.org/10.1016/j.chemgeo.2003.09.009.

Henrie T., Steinpress M., Auckly C., Simion V. and Weber J., 2004. Naturally occurring chromium (VI) in groundwater. In Chromium (VI) Handbook, CRC Press, 442 pp.

Hounslow A.W., 1995. Water Quality Data: analysis and interpretation. CRC Press. USA., 416 pp.

Izbicki J.A., Ball J.W., Bullen T.D. and Sutley S.J., 2008. Chromium, chromium isotopes and selected trace elements, western Mojave Desert. USA. Appl. Geochem., 23: 1325-1352. https://doi.org/10.1016/j.apgeochem.2007.11.015.

Jabari A.R., 1997. Geology and petrology of ophiolite in north Naeen. M. Sci. Thesis., Dept. of Geol., Univ. Isfahan, Iran, 230 pp.

Kaprara E., Kazakis N., Simeonidis K., Coles S., Zouboulis A.I., Samaras P. and Mitrakas M., 2015. Occurrence of Cr(VI) in drinking water of Greece and relation to the geological background. J. Hazard. Mater., 8 (281): 2-11. https://doi.org/10.1016/j.jhazmat.2014.06.084.

Kazakis N., Kantiranis N., Voudouris K.S., Mitrakas M., Kaprara E. and Pavlou A., 2015. Geogenic Cr oxidation on the surface of mafic minerals and the hydrogeological conditions influencing hexavalent chromium concentrations in groundwater. Sci. Total Environ., 514: 224-238. https://doi.org/10.1016/j.scitotenv.2015.01.080.

Kazakis N., Kantiranis N., Kalaitzidou K., Kaprara M., Mitrakas M., Frei R., Vargemezis G., Tsourlos P., Zouboulis A. and Filippidis A., 2017. Origin of hexavalent chromium in groundwater: The example of Sarigkiol Basin, Northern Greece Sci. Total Environ., 593-594: 552-566. https://doi.org/10.1016/j.scitotenv.2017.03.128 .

Kelepertzis E. and Tziritis E., 2015. Assessing the hydrogeochemistry of groundwaters in Ophiolite areas of Euboea Island, Greece, using multivariate statistical methods. J. Geochem. Explor., 159: 79-92. https://doi.org/10.1016/j.gexplo.2015.08.007.

Khaledi Z. and Mohammadzadeh H., 2012. Evaluation of ophiolites and groundwater Chromium and its environmental pollution potential in southeast of Birjand. Journal Econ. Geol., 4 (2): 335-350. https://doi.org/10.22067/ECONG.V4I2.16500.

Lelli M., Grassi S., Amadori M. and Franceschini F., 2014. Natural Cr (VI) contamination of groundwater in the Cecina coastal area and its inner sectors (Tuscany, Italy). Environ. Earth Sci., 71: 3907-3919. https://doi.org/10.1007/s12665-013-2776-2.

Lods G., Roubinet D., Matter J., Leprovost R. and Gouze P., 2020. Groundwater flow characterization of an ophiolitic hard-rock aquifer from cross-borehole multi-level hydraulic. J. Hydrol, 589 (B4). https://doi.org/10.1016/j.jhydrol.2020.125152.

Majidi H., Mahmmodi M.H., Minaei M. and Malekzadeh A., 2019. GQI groundwater quality index in GIS environment, Afcheng ophiolitic area, north of Sabzevar. National Conference of GIscience, Frdowsi Univ., pp. 28-34.

Mardani T., 2018. Geochemistry and quality of groundwater resources in Dasht Baft, southwest of Kerman in relation to ophiolitic masses. 11th National Geological Conference, Qom Payame Noor Univ., pp. 214-229.

Margiotta S., Mongelli G., Summa V., Paternoster M. and Fiore S., 2012. Trace element distribution and Cr (VI) speciation in Ca-HCO_3 and Mg-HCO_3 spring waters from the northern sector of the Pollino Massif, Southern Italy. J. Geochem. Explor., 115: 1-12. https://doi.org/10.1016/j.gexplo.2012.01.006.

Mehdipour Ghazi J., Moazzen M., Rahghoshay M. and Shafaii Moghadam H., 2011. The geodynamic setting of the nain ophiolites, central iran: evidence from chromian spinels in the chromitites and associated rocks. Ofioliti, 36 (1): 59-76.

Mills C.T., Morrison J.M., Goldhaber M.B. and Ellefsen K.J., 2011. Chromium (VI) generation in vadose zone soils and alluvial sediments of the southwestern Sacramento Valley, CA: a potential source of geogenic Cr(VI) to groundwater. Appl. Geochem., 26: 1488-1501. https://doi.org/10.1016/j.apgeochem.2011.05.023.

Moghadam H.S., Corfu F. and Stern R.J., 2013. U-Pb zircon ages of Late Cretaceous Nain - Dehshir ophiolites, Central Iran. J. Geol. Soc., 170: 175-184. https://doi.org/10.1144/jgs2012-066.

Moghadam H.S., Whitechurch H., Rahgoshay M. and Monsef I., 2009. Significance of Nain-Baft ophiolitic belt (Iran): Short-lived, transtensional Cretaceous back-arc oceanic basins over the Tethyan subduction zone. C. R. Geosci., 341: 1016-1028.

Moraetis D., Nikolaidis N.P., Karatzas G.P., Dokou Z., Kalogerakis N., Winkel L.H.E., and Palaiogianni-Bellou A. 2012. Origin and mobility of hexavalent chromium in North-Eastern Attica, Greece. Appl. Geochem., 27: 1170-1178. https://doi.org/10.1016/j.apgeochem.2012.03.005.

Naseem S., Hamza S. and Bashir E, 2010. Groundwater geochemistry of winder agricultural farms, Balochistan, Pakistan and Assessment for Irrigation Water Quality. Eur. Water, 31: 21-32.

Ndung'u K., Friedrich S., Gonzalez A.R. and Flegal, A.R., 2010. Chromium oxidation by manganese (hydr)oxides in a California aquifer. Appl. Geochem., 25: 377-381.

Neal C. and Shand P., 2010. Spring and surface water quality of the Cyprus ophiolites. Hydrology and Earth System Sci., 6 (5): 797-817. https://doi.org/10.5194/hess-6-797-2002.

Nematollahi M.J., Ebrahimi P., Razmara M. and Ghasemi A., 2016. Hydrogeochemical investigations and groundwater quality assessment of Torbat-Zaveh plain, Khorasan Razavi, Iran. Environ. Monit. Assess., 188 (2). https://doi.org/10.1007/s10661-015-4968-6.

Nikic Z., Batoćanin S.D. and Burazer B., 2013. A conceptual model of mildly alkaline water discharging from the Zlatibor ultramafic massif, western Serbia. Hydrogeol. J., 21: 1147-1163. https://doi.org/10.1007/s10040-013-0983-2.

Paternoster M., Rizzo G., Sinisi R., Vilardi G., Di Palma L. and Mongelli G., 2021. Natural hexavalent chromium in the Pollino Massif groundwater (Southern Apennines, Italy): Occurrence, geochemistry and preliminary remediation tests by means of innovative adsorbent nanomaterials. Bull. environ. Contamin. Toxicol., 106: 421-427. https://doi.org/10.1007/s00128-020-02898-7.

Pyrgaki K., Argyraki A., Botsou F., Kelepertzis E., Paraskevopoulou V., Karavoltsos S. and Dassenakis E., 2021. Hydrogeochemical investigation of Cr in the ultramafic rock-related water bodies of Loutraki basin, Northeast Peloponnese, Greece. Environ. Earth Sci., 80: 1-18. https://doi.org/10.1007/s12665-020-09342-3.

Reuter M., Piller W.E., Harzhauser M., Mandic O., Berning B., Rögl F. and Hamedani A., 2009. The Oligo-/Miocene Qom Formation (Iran): evidence for an early Burdigalian restriction of the Tethyan Seaway and closure of its Iranian gateways. Intern. J. Earth Sci., 98: 627-650.

Robertson F.N., 1975. Hexavalent chromium in the ground water in Paradise Valley, Arizona. Ground Water, 13: 516-527.

Robles-Camacho J. and Armienta M.A., 2000. Natural chromium contamination of groundwater at León Valley, México. J. Geochem. Explor., 68: 167-181.

Saputro S., Yoshimura K., Matsuoka S., Takehara K., Narsito Aizawa J. and Tennichi Y., 2014. Speciation of dissolved chromium and the mechanisms controlling its concentration in natural water. Chem. Geol., 364: 33-41. https://doi.org/10.1016/j.chemgeo.2013.11.024.

Stocklin J., 1968. Structural history and tectonics of Iran, a review. Am. Ass. Petrol. Geol. Bull., 52 (7): 1229-1258.

Stumm W. and Morgan J.J., 1996. Aquatic chemistry: chemical equilibria and rates in natural waters, 3rd Ed., Wiley, New York, 1040 pp.

Takin M. and Furnes H., 1972. Iranian geology and continental drift in the Middle East. Nature, 235: 147-150.

Todd D. and Mays L., 2005. Groundwater hydrology. 3rd Ed., John Wiley and Sons Inc., 652 pp.

Vankeuren P., Mateer J., Stute M. and Kelemen P., 2019. Multitracer determination of apparent groundwater ages in peridotite aquifers within the Samail ophiolite, Sultanate of Oman. Earth Planet. Sci. Lett., 516: 37-48. https://doi.org/10.1016/j.epsl.2019.03.007.

Ward J.H. Jr., 1963. Hierarchical grouping to optimize an objective function. J. Am. Statistic. Ass., 58: 236-244.

Wood W.W., Clark D., Imes J.L. and Councell T.B., 2010. Eolian transport of geogenic hexavalent chromium to ground water. Ground Water, 48: 19 -29.

World Health Organization (WHO), 2022. Guidelines for drinking-water quality. 4th Ed., 1376 pp.

Zamani Z., Mahmmodi M. H. and Mehrzad J., 2018. Qualitative investigation of groundwater sources in Sabzevar ophiolitic area for drinking purposes. New research in the field of environmental science and management conference, Kheradgran Inst., pp. 65-74.

Zharf Aab Tadbir Consulting Engineers, 2018. Report of aquifer granulometry in the study area of Naeen. Regional water company of Isfahan, 218 pp.

Received, May 11, 2023
Accepted, October 15, 2023
First published online, January 2, 2024